energies

MDPI

Article

Effects of Pre-Crosslinking on Space Charge and Breakdown Characteristics of XLPE Cable Insulation

Zhenpeng Zhang [1,2], You Wu [3,*], Chao Fu [2], Shaoxin Meng [1,2], Chao Peng [2], Zhonglei Li [3,*] and Boxue Du [3]

[1] State Key Laboratory of Power Grid Environmental Protection, Wuhan 430073, China; 13971276891@163.com (Z.Z.); shaoxinmeng@163.com (S.M.)
[2] China Electric Power Research Institute, Wuhan 430073, China; chaofu@163.com (C.F.); pengchao@163.com (C.P.)
[3] Key Laboratory of Smart Grid of Education Ministry, School of Electrical and Information Engineering, Tianjin University, Tianjin 300072, China; boxuedu@tju.edu.cn
* Correspondence: wuyou1021@tju.edu.cn (Y.W.); lizhonglei@tju.edu.cn (Z.L.)

Abstract: This study focused on the effect of pre-crosslinking on the electrical properties of XLPE insulation for HVDC cables. The XLPE samples were pre-crosslinked at 140, 150 and 160 °C. The space charge and DC breakdown characteristics of the XLPE samples with and without pre-crosslinking were investigated. The results show that the pre-crosslinked XLPE samples have an obvious space charge injection and transportation, resulting in more severe electric field distortion. Under the electric field of 100 kV/mm, the electric field distortion rates of the XLPE samples pre-crosslinked at 150 and 160 °C reached 51% and 72% respectively, which were much higher than that of the XLPE sample without pre-crosslinking (14%.) Compared with the XLPE without pre-crosslinking, the breakdown strengths of XLPE pre-crosslinked at 140, 150 and 160 °C were reduced by 11%, 6% and 7% respectively, at the temperature of 50 °C. It is concluded that the pre-crosslinking leads to imperfect crystallization and micro-defects in the amorphous region of XLPE, thereby leading to more space charge accumulation and reduced DC breakdown. The pre-crosslinking of XLPE insulation therefore should be prevented during HVDC cable manufacturing.

Keywords: HVDC cable; XLPE insulation; space charge; breakdown strength

Citation: Zhang, Z.; Wu, Y.; Fu, C.; Meng, S.; Peng, C.; Li, Z.; Du, B. Effects of Pre-Crosslinking on Space Charge and Breakdown Characteristics of XLPE Cable Insulation. *Energies* **2022**, *15*, 2360. https://doi.org/10.3390/en15072360

Academic Editor: Pawel Rozga

Received: 13 February 2022
Accepted: 22 March 2022
Published: 24 March 2022

1. Introduction

As a basic requirement of economic development, the electric power industry plays an irreplaceable role in human life. However, there is a contradiction between supply and demand in the power industry, and the generation of high-voltage direct current (HVDC) transmission provides a new option to solve this problem. It is worth noting that the insulation problem has always been a key problem that has restricted the development of greater transmission capacity and grades. Due to their advantages of long distance, large capacity and low loss, high-voltage submarine cables are an economical and effective method to transmit power to islands or offshore platforms, and to achieve grid connection of offshore wind power stations and interconnection of power grids [1–3]. The manufacture of long-distance submarine cables can greatly improve the production efficiency, reduce energy consumption, and reduce the number of factory connectors, thereby reducing the impact of factory soft joints on cable insulation performance [4–6]. The main insulation material of high-voltage cable is crosslinked polyethylene (XLPE), which is produced by crosslinking polyethylene material. In the process of crosslinking, peroxide dissociates at high temperature to form free radicals, the molecular chains of polyethylene can be connected to each other in the form of crosslinking bonds, and their molecular structure changes from a linear structure to a three-dimensional network structure. This process also improves the overall heat resistance, dielectric properties and mechanical properties of insulating materials [7–9]. However, in the 30-day continuous production process of

high-voltage submarine cables, it is inevitable that the local extrusion temperature is too high or the time is too long. Therefore, the crosslinking agent will be thermally decomposed in advance under the action of high temperature in the extrusion process, resulting in the pre-crosslinking of XLPE insulation [10,11]. The pre-crosslinked product of XLPE insulation can generate gel, which blocks the filter screen of the extruder, thereby further affecting the rheological properties during the insulation extrusion [12]. In addition, part of the pre-crosslinked product may pass through the filter screen of the extruder into the cable insulation, resulting in inherent defects in the insulation of the HV cable [13]. Therefore, it is crucial to study the effect of pre-crosslinking on the electrical properties of cable insulation.

Space charge characteristics and DC breakdown characteristics are the key properties for HVDC cable insulation that influence the reliability of cable insulation [14–16]. The production process of XLPE cable successively includes the production steps of extrusion molding, high-temperature crosslinking, cooling and degassing [17]. Among these, in the research on the latter two steps, scholars in related fields have conducted a large number of experimental studies. For the high-temperature crosslinking process, Liao et al. investigated the effect of the concentration of DCP agents on the space charge accumulation, and found the increased crosslinking degree can effectively increase the electric field threshold for space charge injection, thereby suppressing the injection of space charges into XLPE insulation [18]. Zhong et al. researched the influence of the crystal and crosslinked morphology on the breakdown strength of XLPE insulation for submarine cable factory joints. It was demonstrated that there is an increase in the content of crosslinked by-products and a reduction in grain size and crystallinity in the XLPE insulation of factory joints, thereby resulting in a lower breakdown strength than that of the cable bulk insulation [19]. Regarding the process of cooling and degassing, Zhou et al. studied the effect of the non-isothermal crystallization process on the onset and motility of positive space charge packets in low density polyethylene (LDPE). The results show that LDPE with a lower cooling rate has higher crystallinity and trap depth, resulting in a lower charge motility and the accumulation of a large number of space charges [20]. Yin et al. found that prolonging the degassing time can effectively reduce the by-products of DCP and inhibit the ionized heterocharges, thereby improving the space charge characteristics of XLPE cable insulation [21]. However, the influence of extrusion temperature on the insulation properties of materials in the extrusion molding stage is often ignored. In view of the fact that insufficient experimental exploration of the process of material pre-crosslinking has been undertaken, the influence of this process on XLPE insulation performance, and its mechanism, are not clear.

This study investigated the effect of pre-crosslinking on the electrical properties of XLPE insulation for HVDC cables. The XLPE samples were pre-crosslinked at 140, 150 and 160 °C. The space charge and DC breakdown characteristics of the XLPE samples with and without pre-crosslinking were investigated, and the effects of crystallinity and crystal morphology on the space charge and breakdown strength were analyzed.

2. Materials and Methods

2.1. Materials

The raw material was supplied by Borealis Company (Vienna, Austria) and had a density of ~0.92 g/cm^3, and mainly contained low-density polyethylene (LDPE), dicumyl peroxide (DCP) and anti-oxide agents. In this study, the pre-crosslinking temperature of XLPE insulating material was set at 140, 150 and 160 °C, followed by high temperature crosslinking at 180 °C. The specific steps were as follows. The XLPE was melted at a temperature of 120 °C for 10 min. Then, the pre-crosslinking process was carried out at 140, 150 and 160 °C, while maintaining the pressure at 15 MPa for 15 min. After the pre-crosslinking, the samples were fully cured for 15 min at a temperature of 180 °C and a pressure of 15 MPa. All the above tests were carried out in a flat vulcanizer. Using this method, sheet XLPE insulation materials with thicknesses of 100 and 200 μm were prepared. To eliminate the by-products of crosslinking, the prepared materials were put in a vacuum

chamber at a temperature of 80 °C for 48 h before testing. In addition, the XLPE without pre-crosslinking was prepared as a reference. These samples were melted at a temperature of 120 °C for 10 min, and then crosslinked at a temperature of 180 °C and a pressure of 15 MPa for 15 min

2.2. Methods

In order to analyze the effect of pre-crosslinking temperature on the crystallization of XLPE insulation, a scanning electron microscope (SEM, Merlin Compact, ZEISS Company of Germany) was employed to observe the spherulite morphology of the XLPE samples after surface etching. The surface-etching process was carried out in a mixed solution of 98% concentrated sulfuric acid solution and potassium permanganate powder (95 and 5 mass parts, respectively) for 4 h. The etched XLPE samples were cleaned with deionized water to remove impurities on the surface of the samples, so as to avoid affecting the SEM images.

The pulse electroacoustic (PEA) method was employed to investigate the space charge behavior of the XLPEs. The HV electrode is a semiconducting layer, and the ground electrode is aluminum. The specific settings of the PEA experimental equipment can be found in our previous paper [22]. The 10 min polarization experiment at −75, −100 and −125 kV/mm, and the 10 min depolarization experiments, were carried out at room temperature for each sample. Furthermore, in order to ensure the repeatability of the experiment and the validity of the data, each group of samples was tested 3 times during the experiment.

Breakdown strength experiments were carried out using a system comprising a pair of ball-plate electrodes at 30, 50 and 70 °C [23]. The high-voltage upper ball-plate electrode is a copper sphere with a radius of 12.5 mm, the grounded lower electrode is a copper circular plate with a radius of 17.5 mm, the edge chamfer is an arc with a radius of 12.5 mm, and the upper and lower electrodes are coaxial. To prevent flashover during voltage boost, the XLPEs and electrodes were dipped in insulating oil. A DC power source with a ramping speed of 1 kV/s was used for this measurement. The tests were repeated 15 times for each material, and the test results were analyzed using the Weibull distribution.

The two-parameter Weibull distribution can be expressed as:

$$P(E) = 1 - \exp\left[-\left(\frac{E}{\alpha}\right)^{\beta}\right] \quad (1)$$

where α is the scale parameter, indicating the corresponding DC breakdown field strength value when the breakdown probability is 63.2%, and β is the shape parameter, which is inversely related to the data dispersion. E represents the breakdown strength.

3. Results

3.1. Effect of Pre-Crosslinking on Crystallization

Figure 1 shows the SEM images of surface-etched XLPE samples with and without pre-crosslinking. It can be seen from the SEM images that the microscopic crystal morphology of the XLPE samples with different components can be clearly observed. By comparing the crystallization of XLPE samples with different pre-crosslinking temperatures, it can be found that the spherulite size of the samples pre-crosslinked at 140 °C (Figure 1a) is significantly smaller than that of the other two groups of pre-crosslinked XLPE samples and normal crosslinked samples. The spherulite size of the pre-crosslinked XLPE samples at 150 and 160 °C increased to a certain extent compared with the pre-crosslinked samples at 140 °C due to the increase in the pre-crosslinking temperature. At the same time, the dispersion of the spherulite size was also increased accordingly. From the images, it can also be seen that the amorphous region accounts for a large area in the microstructure of the sample, which leads to a larger interval width between adjacent spherulites.

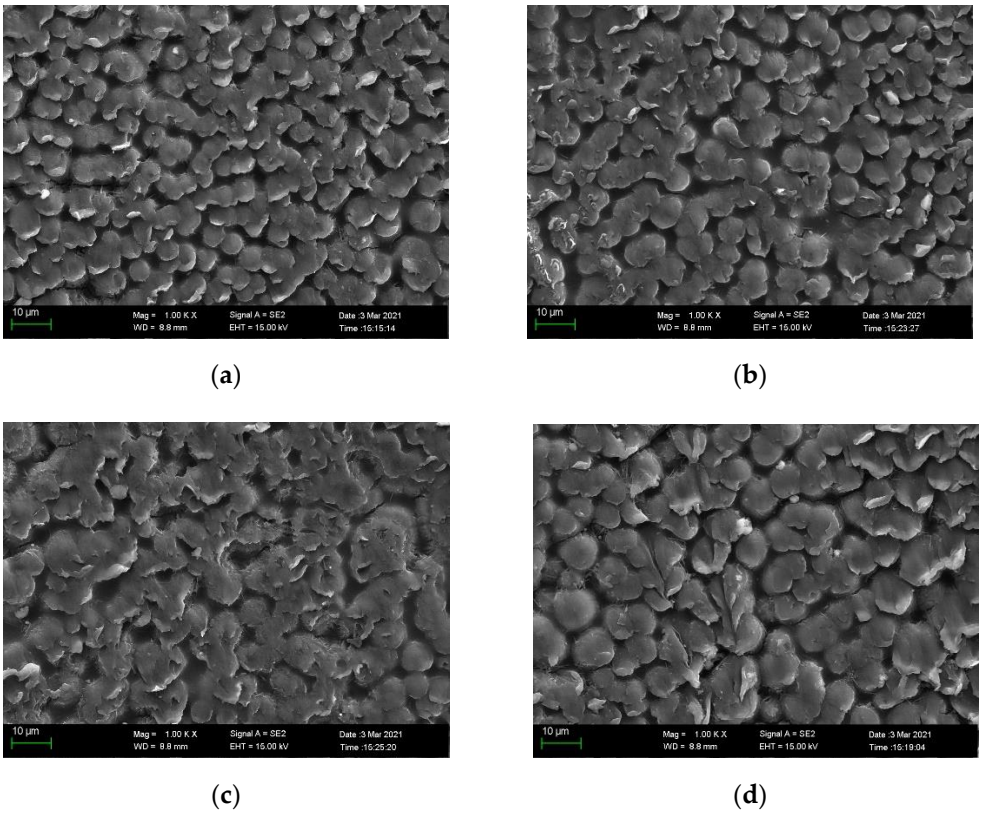

Figure 1. SEM images of surface-etched XLPE samples: (**a**) pre-crosslinked XLPE at 140 °C; (**b**) pre-crosslinked XLPE at 150 °C; (**c**) pre-crosslinked XLPE at 150 °C; (**d**) XLPE without pre-crosslinking.

Compared with the pre-crosslinked XLPEs, the spherulite size of the XLPE sample without pre-crosslinking is relatively uniform, and the spherulites are closely arranged. Additionally, the distance between the spherulites is small, and the area ratio of the amorphous region is relatively small. Therefore, the crystal structure of the normally crosslinked XLPE insulating sample is relatively more complete.

The differential scanning calorimetry (DSC) test was employed to characterize the crystallinity of the bulk XLPE samples. The crystallinity of the insulation with pre-crosslinking temperatures of 140, 150, and 160 °C was 30.7%, 26.8% and 26.7%, respectively. These value were significantly lower than that of the XLPE without pre-crosslinking (34.3%). The crystallinity results obtained by the DSC test are consistent with the SEM images.

3.2. Effect of Pre-Crosslinking on Space Charge Behaviors

Figure 2 shows the space charge characteristics and electric field distributions of the XLPE samples under the DC electric field of −75 kV/mm at room temperature of 30 °C. It can be seen from Figure 2 that, compared with the XLPE without pre-crosslinking, an obvious injection of space charge packets occurs in the pre-crosslinked XLPE samples during the polarization process. Under the action of an external electric field, a large number of same-polarity charges are injected from the anode side of the pre-crosslinked XLPE sample. With the polarization process, the positive charge moves towards the cathode in the form of charge packets until it migrates near the cathode and is extracted from the cathode. Among the pre-crosslinked XLPEs, the injection and migration of space charge packets in the XLPE pre-crosslinked at 140 °C were the most obvious, with the highest space charge density. Additionally, the migration process of two space charge packets appeared after 300 s, whereas only one space charge packet was injected in the pre-crosslinked XLPE samples at 150 °C and 160 °C.

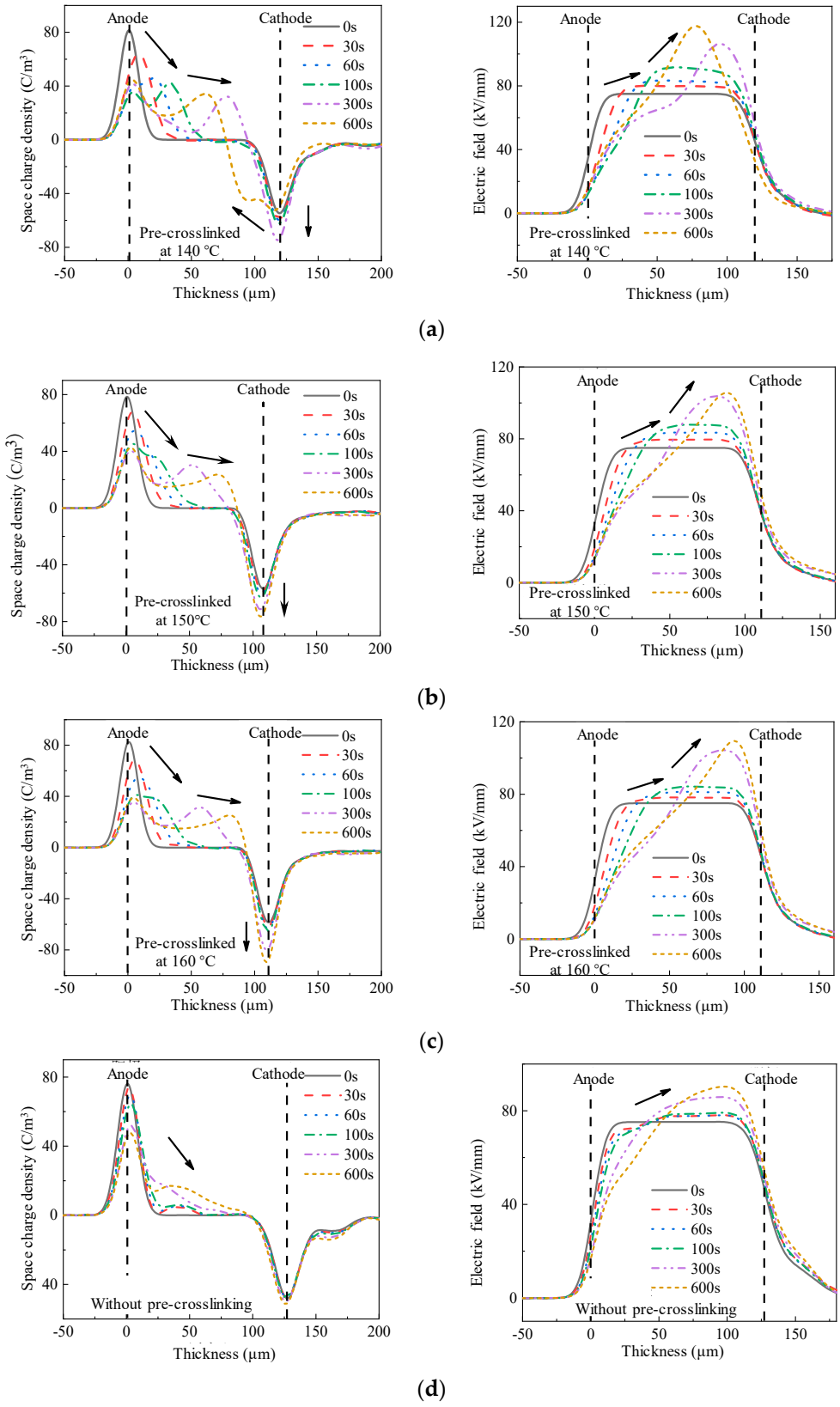

Figure 2. Space charge characteristics and electric field distributions of the XLPE sample under the DC electric field of −75 kV/mm at a test temperature of 30 °C: (**a**) XLPE pre-crosslinked at 140 °C; (**b**) XLPE pre-crosslinked at 150 °C; (**c**) XLPE pre-crosslinked at 160 °C; (**d**) XLPE without pre-crosslinking.

The injection and migration of space charge packets also led to the occurrence of local field intensity distortion inside the pre-crosslinked XLPE samples. Due to the injection of the same polarity charge near the anode, an induced electric field opposite to the applied electric field is generated, thereby weakening the electric field strength near the anode. The migration process of the space charge packets leads to the enhancement of the local electric field strength inside the insulating sample, and with the migration direction of the charge packets, the enhancement of the local electric field gradually moves from the anode to the cathode.

Figure 3 shows the space charge characteristics and electric field distributions of the XLPE samples under the DC electric field of −100 kV/mm at room temperature of 30 °C. It can be seen that the injection of space charge packets in the pre-crosslinked XLPE samples under the −100 kV/mm DC electric field is more evident than that under the −75 kV/mm DC electric field. The increase in the amount of charge injected from the anode leads to a significant increase in the amplitude of the charge density of the injected space charge packets inside the sample. When the polarization time is 100 s, the maximum density of space charge packet of the XLPE pre-crosslinked at 140 °C is only 40 C/m^3 under −75 kV/mm, whereas the space charge density amplitude under −100 kV/mm reaches 120 C/m^3. Additionally, an apparent negative space charge packet injection occurs at the electric field of −100 kV/mm as the polarization time is 300 s.

By comparison, the injection depth and migration speed of space charge packets inside the medium also increase significantly with the increase in the electric field. When the polarization time was 300 s, the migration distance of the charge packets of the pre-crosslinked XLPE samples at 140 °C was 85 μm under −75 kV/mm, and did not migrate to the cathode. However, under the DC electric field of −100 kV/mm, the first charge packet appearing in the medium migrated to and was extracted from the cathode, and the injection of the second space charge packet also occurred.

The increase in the amplitude of the charge density of the injected charge packet in the insulating sample also caused more serious local electric field distortion in the sample. Compared with the XLPE samples without pre-crosslinking, the 150 and 160 °C pre-crosslinked XLPE samples underwent obvious electric field distortion near the cathode with the migration of charge packets, and the maximum electric field appeared in both cases at the polarization time of 600 s. The electric field distortion rate is employed to characterize the time-dependent electric field distribution inside the sample, which is defined as follows [24]:

$$\delta = \frac{|E_{max} - E_0|}{E_0} \times 100\% \quad (2)$$

where E_{max} is the maximum electric field strength distorted by the space charge. E_0 is the average value of the applied field. The electric field distortion rates of the 150 and 160 °C pre-crosslinked XLPE samples reached 51% and 72%, respectively, which are much higher than that of XLPE sample without pre-crosslinking (14%).

Figure 4 presents the space charge and electric field distributions of XLPE samples under a DC electric field of −125 kV/mm at 30 °C. Under the DC electric field of −125 kV/mm, the space charge packets injected into the pre-crosslinked XLPE samples not only increased the amplitude of the space charge packets, but also increased their width. From the migration process of the space charge packets in the pre-crosslinked XLPE medium at 140 °C, it can be observed that the migration speed of the injected positive charge packets gradually slows during the process of migrating from the anode to the cathode under the action of an external electric field. The reason for this phenomenon is that the electrons inside the medium migrate from the cathode to the anode under the action of the external electric field, whereas the positive space charge packets migrate from the anode to the cathode. The electrons recombine with positive charges, resulting in a slowing of the migration of space charge packets [25]. Compared with other XLPE insulation samples, multiple injections of positive space charge packets appeared in the XLPE pre-crosslinked at 140 °C.

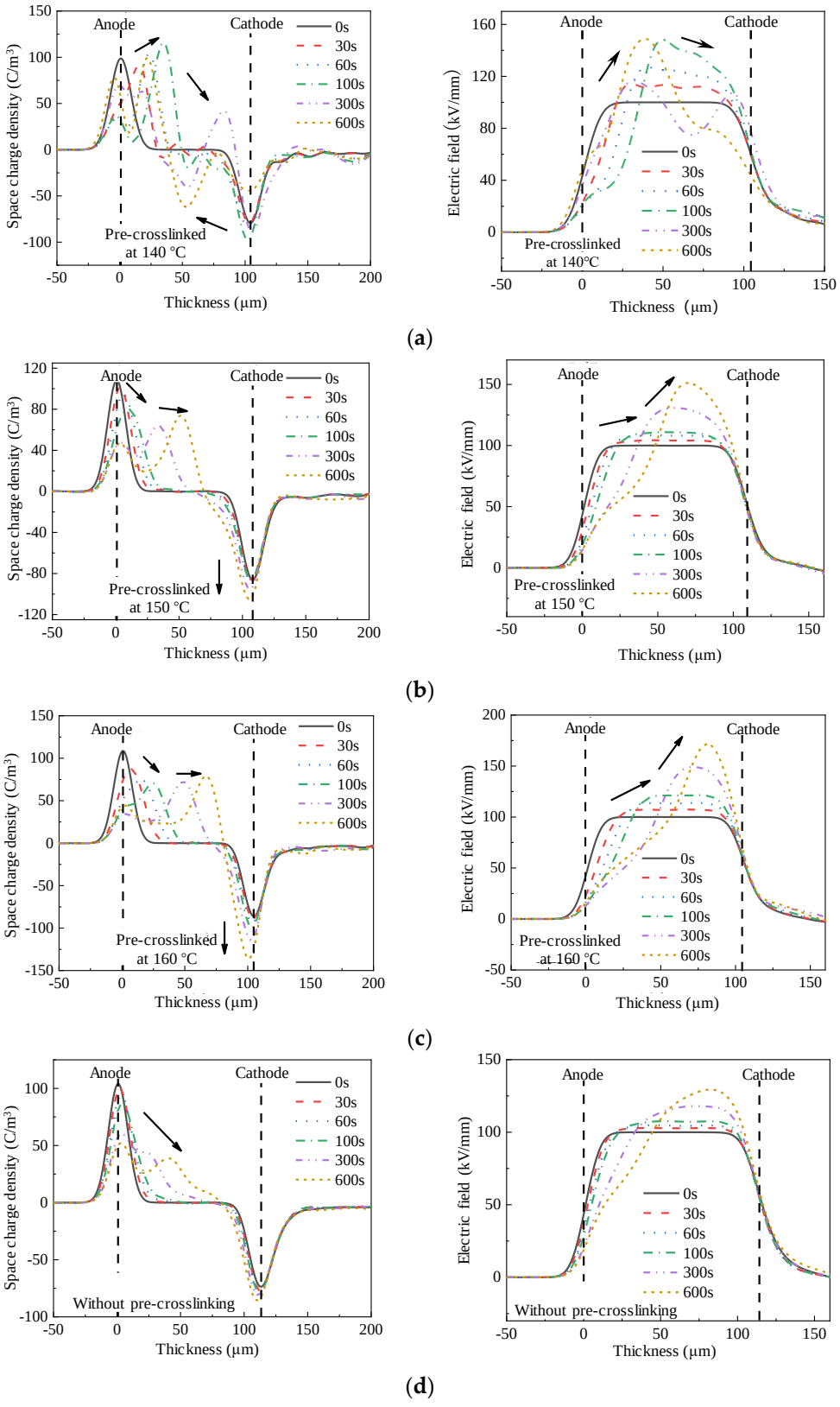

Figure 3. Space charge characteristics and electric field distributions of the XLPE sample under the DC electric field of −100 kV/mm at a test temperature of 30 °C: (**a**) XLPE pre-crosslinked at 140 °C; (**b**) XLPE pre-crosslinked at 150 °C; (**c**) XLPE pre-crosslinked at 160 °C; (**d**) XLPE without pre-crosslinking.

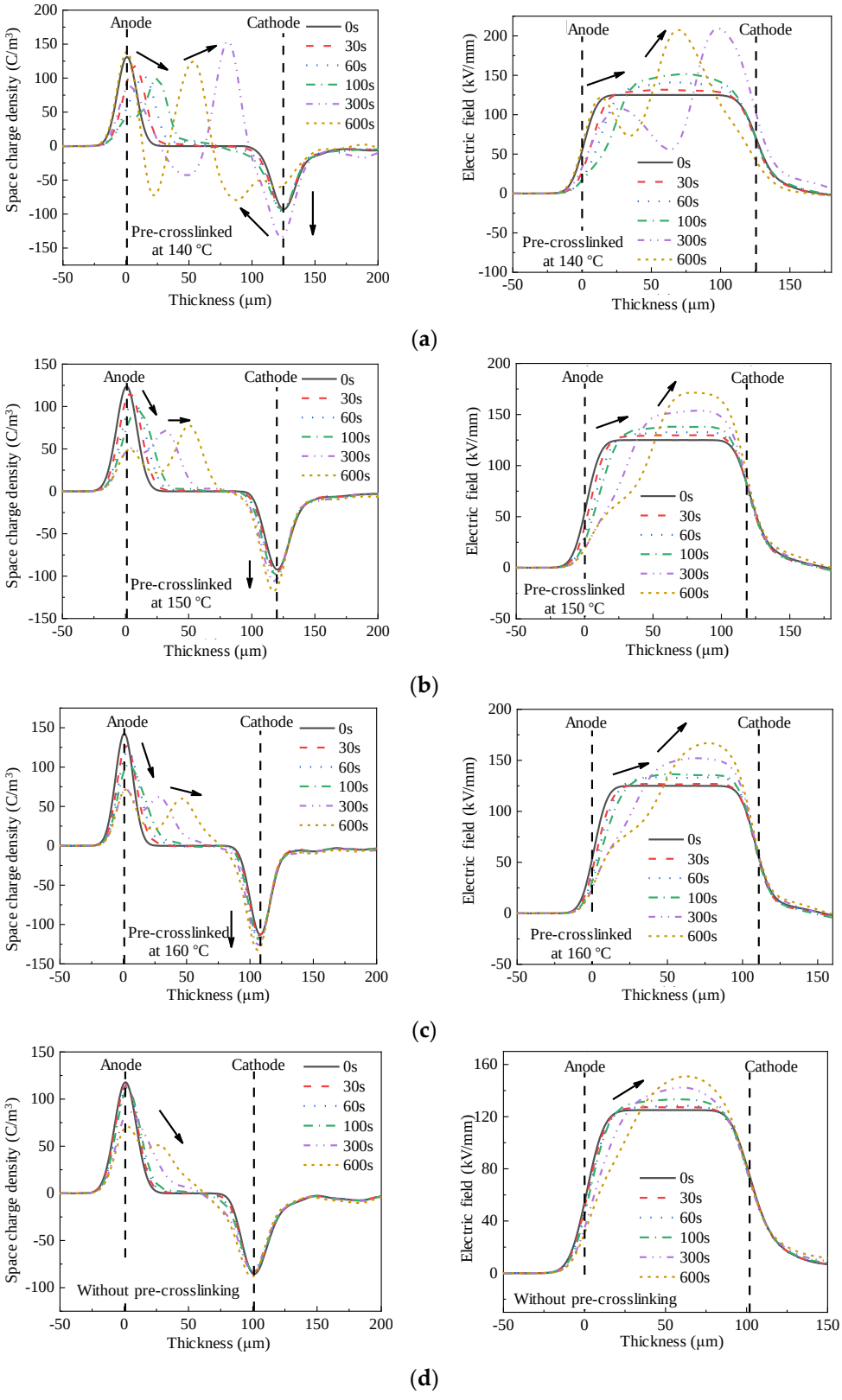

Figure 4. Space charge characteristics and electric field distributions of the XLPE sample under the DC electric field of −125 kV/mm at a test temperature of 30 °C: (**a**) XLPE pre-crosslinked at 140 °C; (**b**) XLPE pre-crosslinked at 150 °C; (**c**) XLPE pre-crosslinked at 160 °C; (**d**) XLPE without pre-crosslinking.

It is concluded that the pre-crosslinked XLPE samples significantly enhance the space charge injection, which has a serious impact on the electric field distortion and insulation aging during the operation of the DC cable.

3.3. Effect of Pre-Crosslinking on Breakdown Strength

Figure 5 shows the Weibull distributions of the DC breakdown strength of XLPE samples at 30, 50 and 70 °C. It can be seen that under any temperature condition, the breakdown field strength of the pre-crosslinked XLPE sample decreases significantly compared with the normal XLPE sample. Among the samples, the breakdown field strength of the pre-crosslinked XLPE sample at 140 °C is the lowest, mainly resulting from its lower degrees of crosslinking and crystallinity. The breakdown first occurred at the micro-defect inside the amorphous region, resulting in a lower breakdown field strength of the specimen compared to the other groups of XLPE specimens [26].

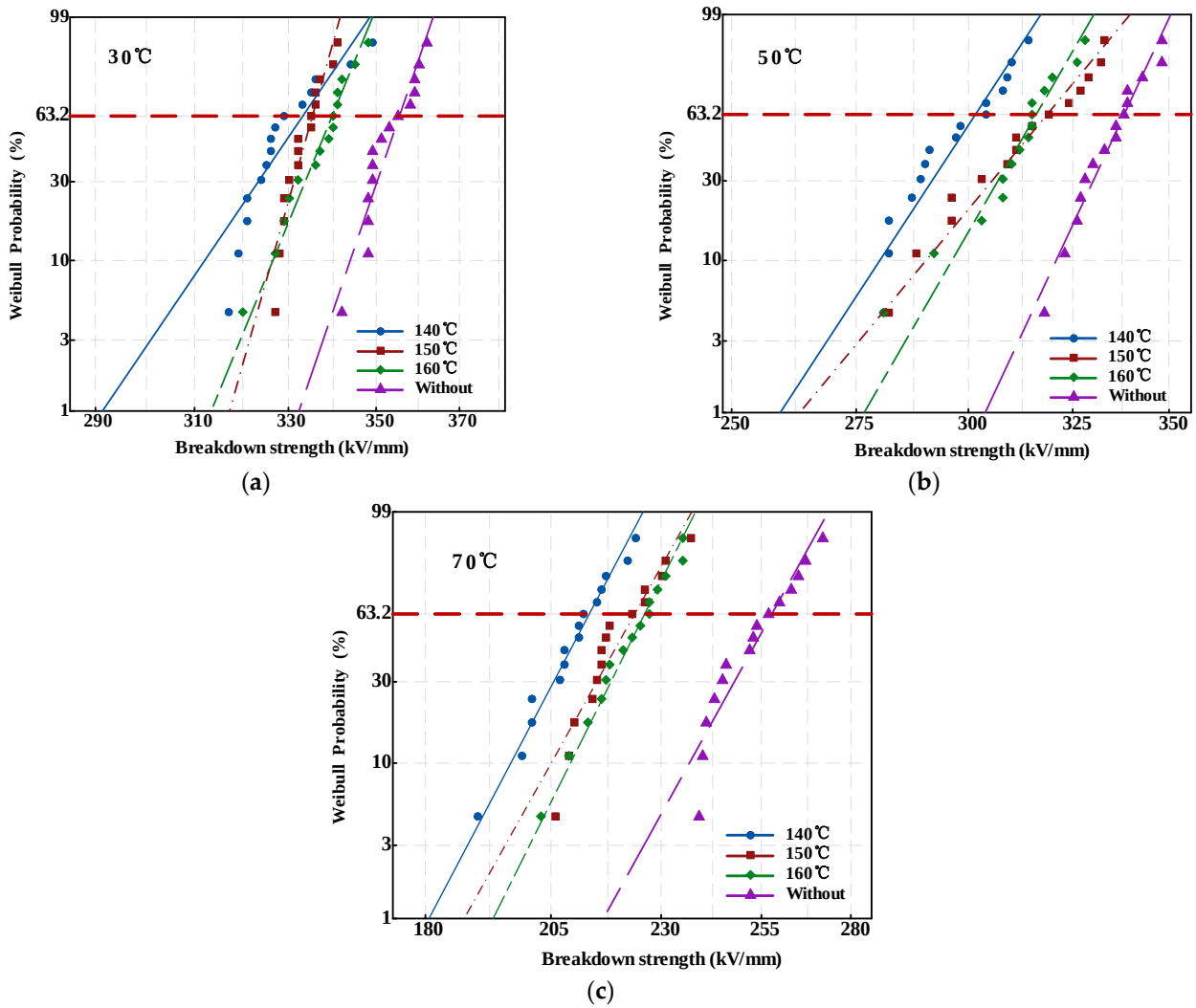

Figure 5. Weibull distributions of the breakdown strength of XLPE samples under the temperature of: (**a**) 30 °C; (**b**) 50 °C; (**c**) 70 °C.

Table 1 shows the Weibull parameters of the breakdown strength of XLPE samples at different temperatures. It can be seen that under the test temperature condition of 50 °C, the scale parameters of the breakdown strength of XLPE pre-crosslinked at 140, 150 and 160 °C were reduced by 11%, 6% and 7%, respectively, compared with the samples without pre-crosslinking. The results of the breakdown strength test show that the existence of

the pre-crosslinking process results in defects in the crosslinking structure and crystalline morphology of the sample, resulting in a decrease in the dielectric strength of the XLPE sample. It also can be seen that, with the increase in temperature, the scale and shape parameters of XLPEs both decreased. Compared with the XLPE without pre-crosslinking, the increase in temperature has a more significant effect on the electrical strength of the pre-crosslinked XLPE.

Table 1. Weibull parameters of the breakdown strength of XLPE samples at different temperatures.

Temperature (°C)	Pre-Crosslinking Temperature (°C)	SCALE Parameter α (kV/mm)	Shape Parameter β
30	140	333.4	34.20
	150	335.4	82.56
	160	339.8	57.00
	Without pre-crosslinking	355.5	68.22
50	140	301.7	30.50
	150	318.9	24.10
	160	316.1	34.64
	Without pre-crosslinking	338.3	42.94
70	140	213.5	27.58
	150	223.9	25.91
	160	226.1	29.26
	Without pre-crosslinking	258.2	26.18

Under the test temperature condition of 30 °C, the dimension parameters of XLPE pre-crosslinked at 140 °C are 6% lower than those of normal XLPE. At the test temperature of 70 °C, the dimensional parameters of the XLPE pre-crosslinked at 140 °C decreased by 17% compared with the normal XLPE. With the increase in the ambient temperature, the electrical strength of the pre-crosslinked sample decreased by a higher percentage than that of the XLPE without pre-crosslinking.

Additionally, the shape parameter value of pre-crosslinked XLPE decreased significantly with the increase in temperature. The decrease in the shape parameters indicates that the dispersion of the test data becomes larger, which proves that the pre-crosslinking not only causes the decrease in the electrical strength of XLPE, but also leads to the decrease in the insulation stability of the material. In other words, high temperature causes the micro-defects in the amorphous region of the pre-crosslinked XLPE material to be more prone to breakdown.

4. Discussion

To further analyze the effect of pre-crosslinking on the space charge transportation, the amplitudes and motilities of the space charge packets under different DC electric fields were quantitatively calculated. The solid lines in Figure 6 are the amplitudes of the space charge packets in the bulk of XLPE samples under different electric fields. This shows that the average amplitude of the space charge packets injected into the normal XLPE samples is relatively small, whereas the amplitude of the space charge packets injected into the pre-crosslinked XLPE samples is significantly increased. This is because the pre-crosslinking process causes imperfect crystallization of the XLPE sample, and the micro-defect in the amorphous region increases the probability of the homopolar charges being injected into the XLPE samples. Among the pre-crosslinked XLPE samples, those at 140 °C have the highest amplitude of the injected space charge packets.

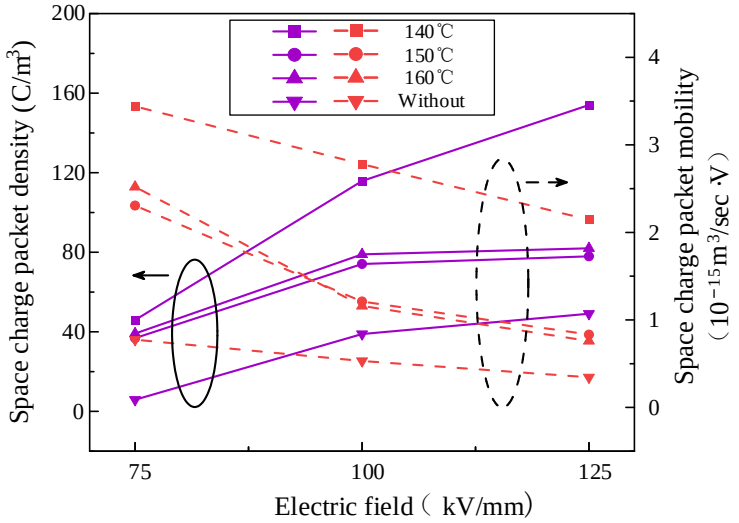

Figure 6. Amplitude and motilities of the space charge package of XLPE samples under different DC electric fields.

It can also be observed that the amplitude of the positive space charge package injected into the sample increases continuously with the increase in the applied electric field strength. For the XLPE sample pre-crosslinked at 140 °C, the average amplitude of the space charge inside the dielectrics is only 46 C/m^3 under the DC electric field of −75 kV/mm, but as the electric field intensity increases to −100 and −125 kV/mm, the average amplitudes of the charge packets increased to 116 and 154 C/m^3, respectively.

The space charge packet results in Section 3.2 also indicate the positive charges migrate from the anode to the cathode inside the dielectrics, and the motilities of the space charge packets are not constant. Considering that the space charge packet is a non-uniform transportation process, the motility of a space charge packet is defined as the average value over a period of time, which can be expressed as:

$$M_{SCP} = \frac{L_2 - L_1}{t_2 - t_1} \times \frac{1}{E_{appl}} \quad (3)$$

where t_1 and t_2 correspond to the start and end times of the apparent displacement of the space charge packet, respectively. L_1 and L_2 correspond to the position of the space charge packet at t_1 and t_2, respectively. E_{appl} is the applied electric field.

The motilities of the space charge packets under different DC electric fields are shown by the dashed lines in Figure 6. It can be seen from the figure that the average motility of the charge packets in the normal crosslinked XLPE sample is the lowest, and the average motility is 0.77 × 10^{-15} m^2/s·V under the applied electric field strength of 75 kV/mm. However, the pre-crosslinking process leads to the relatively incomplete crosslinked structure of the sample, which results in a rapid increase in the average motility of the charge package inside the medium. Among the samples, the average motility of the XLPE pre-crosslinked at 140 °C was the highest, and was 3.44 × 10^{-15} m^2/s·V.

Combined with the experimental results in Section 3.1, it is considered that the pre-crosslinking process leads to the reduction in the crystallinity of the XLPE sample and the reduction in the spherulite size, which makes the injection of charge packets more likely to occur inside the sample. As the temperature of the pre-crosslinked XLPE decreases, the larger the average amplitude of the space charge packets injected inside the insulating material, the higher the average motility.

Additionally, the higher the applied electric field strength, the lower the average motility of the charge packets within the sample. This is mainly due to the recombination of heteropolar charges inside the XLPE samples. With the increase in the field strength from 75 to 125 kV/mm, the negative space charge injection phenomenon appears near the

cathode, and the negative space charges migrate from the cathode to the anode under the action of the electric field force. During the migration process, the recombination process of negative and positive space charge packets occurs in the sample, resulting in a decrease in charge motility. It has been proven that the recombination of charge carriers would produce hot electrons due to non-radiative transition of energy via an Auger-type process [27]. The hot electrons may have sufficient energy to collide with a molecule and dissociate into free radicals. This process can be expressed as:

$$\begin{aligned} AB + e^-(\text{hot}) &\rightarrow A^* + B^* + e^-(\text{cold}) \\ \textit{or} &\rightarrow A^* + B^* + e^-(\text{trapped}) + \text{energy release} \end{aligned} \quad (4)$$

The energy released from the charge combination process results in the formation of a low-density region, in which electrons are more easily accelerated by the electric field and gain kinetic energies to cause chain scission. As a result, the chain scissions and micro-defects in amorphous regions may cause partial discharge and further develop into the breakdown of polymer, which contributes to the decrease in breakdown strength [28].

5. Conclusions

This study investigated the effect of pre-crosslinking on space charge and breakdown characteristics of XLPE insulation for HVDC cables. The main conclusions can be summarized as follows:

(1) The pre-crosslinking temperature affects the crystalline morphology of the XLPE samples. With the decrease in the pre-crosslinking temperature, the grain size of the sample gradually decreases, and the spherulite arrangement becomes looser, which leads to decreases in the integrity of the crystalline structure and the crystallinity of the pre-crosslinked XLPE sample.

(2) Compared with the XLPE sample without pre-crosslinking, the pre-crosslinked XLPE is more prone to the injection of charge packets into the bulk due to its imperfect crystalline structure. As the DC electric field increases from 75 to 125 kV/mm, the amplitude of the injected space charge packet increases significantly, resulting in increased electric field distortion.

(3) Pre-crosslinking leads to a significant decrease in the DC breakdown field strength, which is closely related to the imperfect spherulite structure and micro-defects of the XLPE insulation.

Considering the actual operating conditions of the cable, XLPE insulation is not only affected by the electric field, but also by the operating temperature. Comprehensive analysis of the effect of pre-crosslinking on the dielectric properties of materials, such as the space charge under the condition of multi-physics coupling, and exploration of the structure–activity relationship between the microstructure and macroscopic properties of materials, will be the direction and focus of future work.

Author Contributions: Conceptualization, Z.Z., Z.L. and B.D.; methodology, Y.W.; software, Y.W.; validation, Y.W. and Z.Z.; formal analysis, Y.W. and Z.Z.; investigation, Y.W. and Z.Z.; resources, Y.W., Z.Z., C.F., S.M. and C.P.; data curation, Y.W. and Z.Z.; writing—original draft preparation, Z.L. and B.D.; writing—review and editing, Z.L. and B.D.; visualization, Z.L. and B.D.; supervision, Z.Z.; project administration, Z.Z.; funding acquisition, Z.Z. All authors have read and agreed to the published version of the manuscript.

Funding: This research was supported by Open Fund of State Key Laboratory of Power Grid Environmental Protection (China Electric Power Research Institute) (No. GYW51202101371).

Institutional Review Board Statement: Not applicable.

Informed Consent Statement: Not applicable.

Data Availability Statement: Not applicable.

Conflicts of Interest: The authors declare no conflict of interest.

References

1. Zhou, Y.; Yuan, C.; Li, Q.; Wang, Q.; He, J. Recyclable insulation material for HVDC cables in global energy interconnection. *Glob. Energy Interconnect.* **2018**, *1*, 520–526.
2. Li, Z.L.; Du, B.X. Polymeric insulation for high-voltage DC extruded cables: Challenges and development directions. *IEEE Electr. Insul. Mag.* **2018**, *34*, 30–43.
3. Wang, L.; Nguyen Thi, M.S. Comparative Stability Analysis of Offshore Wind and Marine-Current Farms Feeding into a Power Grid Using HVDC Links and HVAC Line. *IEEE Trans. Power Deliv.* **2013**, *28*, 2162–2171.
4. Ye, H.; Fechner, T.; Lei, X.; Luo, Y.; Zhou, M.; Han, Z.; Wang, H.; Zhuang, Q.; Xu, R.; Li, D. Review on HVDC cable terminations. *High Volt.* **2018**, *3*, 79–89.
5. Huang, X.Y. Perspective on emerging materials for high voltage applications. *High Volt.* **2020**, *5*, 229–230.
6. Kubota, T.; Takahashi, Y.; Sakuma, S.; Watanabe, M.; Kanaoka, M.; Yamanouchi, H. Development of 500kV XLPE Cables and Accessories for Long Distance Underground Transmission Line. *IEEE Trans. Power Deliv.* **1994**, *9*, 1741–1749.
7. Vahedy, V. Polymer insulated high voltage cables. *IEEE Electr. Insul. Mag.* **2006**, *22*, 13–18.
8. Smedberg, A.; Gustafsson, B.; Hjertberg, T. What is crosslinked polyethylene? *IEEE Int. Conf. Solid Dielectr.* **2004**, 415–418.
9. Precopio, F. The invention of chemically crosslinked polyethylene. *IEEE Electr. Insul. Mag.* **1999**, *15*, 23–25.
10. China Has Developed the First 500 kV Submarine Cable in the World. Available online: http://www.xinhuanet.com/science/2017-12/04/c_136799927.htm (accessed on 4 December 2017).
11. Zhong, L.; Ren, H.; Cao, L.; Zhao, W.; Gao, J. Development of High Voltage Direct Current Extruded Cables. *High Volt. Eng.* **2017**, *43*, 3473–3489. (In Chinese)
12. Harlin, A. Model for XLPE Runtime Prediction for Single-Screw and Conical Extruder in CV Line. In Proceedings of the 52nd IWCS/Focus International Wire & Cable Symposium, Philadelphia, PA, USA, 17–20 November 2003; Tampere University of Technology: Tampere, Finland, 2003.
13. Tanaka, Y.; Chen, G.; Zhao, Y.; Davies, A.E.; Vaughan, A.S.; Takada, T. Effect of additives on morphologyand space charge accumulation in low density polyethylene. *IEEE Trans. Dielectr. Electr. Insul.* **2003**, *10*, 148–154.
14. Montanari, G.C. Bringing an insulation to failure: The role of space charge. *IEEE Trans. Dielectr. Electr. Insul.* **2011**, *18*, 339–364.
15. Zhang, Y.; Lewiner, J.; Alquie, C.; Hampton, N. Evidence of strong correlation between space charge buildup and breakdown in cable insulation. *IEEE Trans. Dielectr. Electr. Insul.* **1996**, *3*, 778–783.
16. Li, Z.L.; Fan, M.S.; Zhou, S.F.; Du, B.X. BNNS Encapsulated TiO2 Nanofillers Endow Polypropylene Cable Insulation with Enhanced Dielectric Performance. *IEEE Trans. Dielectr. Electr. Insul.* **2021**, *28*, 1238–1246.
17. Hanley, T.L.; Burford, R.P.; Fleming, R.J.; Barber, K.W. A general review of polymeric insulation for use in HVDC cables. *IEEE Electr. Insul. Mag.* **2003**, *19*, 13–24.
18. Zhou, Q.; Wu, N.; Liao, R.J.; Zhong, L.S.; Ren, H.Y.; Cao, L. Space Charge Characteristics of Cross-linked Polyethylene with Different Cross-linking Degrees. *High Volt. Eng.* **2013**, *39*, 294–301.
19. Zhang, Z.; Zhao, J.; Zhao, W.; Zhong, L.; Hu, L.; Rao, W.; Zheng, M.; Meng, S. Influence of Morphological Variations in XLPE on the AC Breakdown Performance of Submarine Cable Factory Joint Insulation. *High Volt.* **2019**, *5*, 69–75.
20. Zahn, Z.; Wang, W.; Ninghua, N.; Sun, S.; Qinghua, Q.; Liang, L.; Xidong, X.; Guan, G.; Zhichen, Z. Morphology effects on space charge characteristics of low density polyethylene. *Jpn. J. Appl. Phys.* **2011**, *50*, 017101.
21. Zhang, H.; Chen, M.; Wang, Y.; Wu, J.; Yin, Y. Interaction Effects of Three Major Crosslinking Byproducts on Space Charge Accumulation in Polyethylene. *IEEE Trans. Dielectr. Electr. Insul.* **2021**, *28*, 710–718.
22. Li, Z.; Du, B.; Han, C.; Xu, H. Trap Modulated Charge Carrier Transport in Polyethylene/Graphene Nanocomposites. *Sci. Rep.* **2017**, *7*, 4015.
23. Zhou, Y.; Hu, J.; Dang, B.; He, J. Mechanism of highly improved electrical properties in polypropylene by chemical modification of grafting maleic anhydride. *J. Phys. D Appl. Phys.* **2016**, *49*, 415301.
24. Cheng, Z.; Zekai, L.U.; Zhang, L. Space Charge Behavior of DC Cable's XLPE Material at High Temperatures. *High Volt. Eng.* **2018**, *44*, 2664–2671.
25. Zhao, J.; Chen, G.; Lewin, P.L. Investigation into the formation of charge packets in polyethylene: Experiment and simulation. *J. Appl. Phys.* **2012**, *112*, 1546–1551.
26. Jones, J.P.; Llewellyn, J.P.; Lewis, T.J. The contribution of Field Induced Morphological Change to the Electrical Aging and Breakdown of Polyethylene. *IEEE Trans. Dielectr. Electr. Insul.* **2005**, *12*, 951–966.
27. Dissado, L.A.; Fothergill, J.C. *Electrical Degradation and Breakdown in Polymers*; Peter Peregrinus: London, UK, 1992.
28. Matsui, K.; Tanaka, Y.; Takada, T.; Fukao, T.; Fukunaga, K.; Maeno, T.; Alison, J.M. Space charge behavior in low-density polyethylene at pre-breakdown. *IEEE Trans. Dielectr. Electr. Insul.* **2005**, *12*, 406–415.